A Journal of the Gesellschaft Deutscher Chemiker

Angewandte International Edition

GDCh

Chemie

www.angewandte.org

Accepted Article

Title: Synergistic Activation of Amides and Hydrocarbons for Direct C(sp3)–H Acylation Enabled by Metallaphotoredox Catalysis

Authors: Geun Seok Lee, Joonghee Won, Seulhui Choi, Mu-Hyun Baik, and Soon Hyeok Hong

To be cited as: *Angew. Chem. Int. Ed.* 10.1002/anie.202004441

Link to VoR: https://doi.org/10.1002/anie.202004441

WILEY-VCH

10.1002/anie.202004441

RESEARCH ARTICLE

WILEY-VCH

Synergistic Activation of Amides and Hydrocarbons for Direct C(sp³)–H Acylation Enabled by Metallaphotoredox Catalysis

Geun Seok Lee,[a][b] Joonghee Won,[a][c] Seulhui Choi,[a][c] Mu-Hyun Baik,*[a][c] and Soon Hyeok Hong*[a]

Abstract: The utilizations of omnipresent, thermodynamically stable amides and aliphatic C(sp³)–H bonds for various functionalizations are ongoing challenges in catalysis. In particular, the direct coupling between the two functional groups has not been realized. Here, we report the synergistic activation of the two challenging bonds, the amide C–N and unactivated aliphatic C(sp³)–H, via metallaphotoredox catalysis to directly acylate aliphatic C–H bond utilizing amides as stable and readily accessible acyl surrogates. N-acylsuccinimides served as efficient acyl reagents for the streamlined synthesis of synthetically useful ketones from simple C(sp³)–H substrates. Detailed mechanistic investigations using both computational and experimental mechanistic studies were performed to construct a detailed and complete catalytic cycle. The origin of the superior reactivity of the N-acylsuccinimides over other more reactive acyl sources such as acyl chlorides was found to be an uncommon reaction pathway which commences with C–H activation prior to oxidative addition of the acyl substrate.

Introduction

The reactivity of carboxylic acid derivatives (RCOY) in conventional addition-elimination reactions is determined by the electronic character of the carbonyl carbon depending on the substituents (Y) and the order of reactivity is well-documented ranging from the most reactive acyl halides to the least reactive amides. Transition metal catalyzed C–Y bond activation reactions generally follow the same trend, where acyl chlorides show practically barrierless oxidative additions and amides are inert to such activation mode.[1] This inertness is ascribed to the exceptional stability of amides due to electronic contribution of the nitrogen lone pair,[2] which participates in a strong π-conjugation with the carbonyl functionality. As a result, the activation of amides via C–N bond cleavage is a challenging topic in transition metal catalysis (Scheme 1a). These difficulties notwithstanding, amides are easy to access and they would make highly desirable substrates serving as an acyl or an alkyl surrogate. Pioneered by Szostak[1,3] and Garg,[4] examples of successful oxidative addition of amide C–N bonds to selected transition metal complexes have appeared,[1, 5] where the ground state destabilization by modifying the stereoelectronic characters of amides was thought to be key.

N-acylimides[6] and amides decorated with electron-withdrawing groups,[7] most representatively phthalimide, Boc or sulfonyl protecting groups, are known to be activated due to their twisted structure that disrupts the aforementioned π-conjugation. Amides based on pyrroles[8] or N-methylaminopyrimidines[9] are also reported to undergo oxidative addition, and Pd, Rh, and Ni were found to be particularly active in various cross-coupling reactions of the stereoelectronically modified amides, enabling alkylation,[10] arylation,[1,7b,11] cyanation,[12] transamidation,[13] esterification,[4] borylation[14], reduction,[15] and other useful transformations.[16] However, in all reactions highly reactive, transmetallating or strongly nucleophilic coupling partners were employed, likely due to the fundamental challenge of the amide activation. The coupling of amides with an unactivated coupling partner such as an aliphatic C(sp³)–H bond without the aid of a directing group remains elusive and poses the additional difficulty of concurrent activation of two notoriously difficult substrate classes (Scheme 1a).

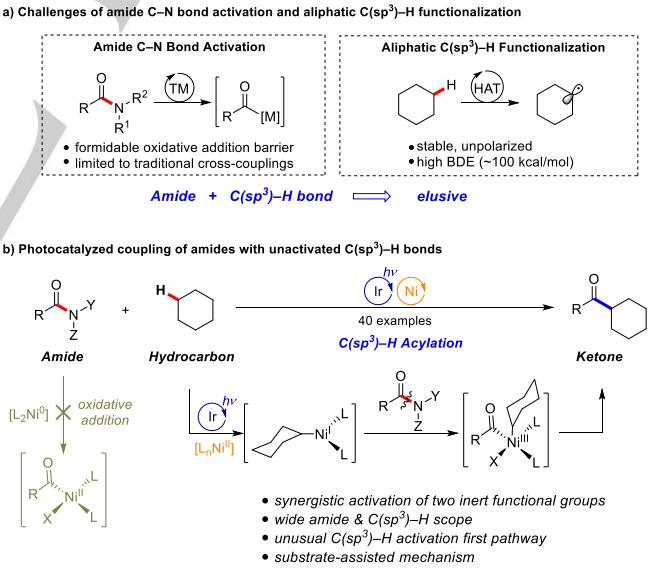

Scheme 1. Amide C–N bond cleavage and merger with C(sp³)–H activation.

We envisioned that the cross coupling of C(sp³)–H bonds with amides may be possible by a dual catalysis strategy utilizing visible light as the driving energy source (Scheme 1b). This work represents the first case of successful C(sp³)–H functionalization with amides as a user-friendly acyl surrogate and a rare example of applying photoredox catalysis in conjunction with amide activation,[17] thus breaking the boundaries of both reaction modes. Namely, a significantly challenging cross-coupling reaction between two inert functional

[a] G. S. Lee, J. Won, S. Choi, Prof. M.-H. Baik, Prof. S. H. Hong
Department of Chemistry
Korean Advanced Institute of Science and Technology (KAIST)
Daejeon 34141, Republic of Korea
E-mail: mbaik2805@kaist.ac.kr
soonhyeok.hong@kaist.ac.kr
[b] G. S.Lee
Department of Chemistry, College of Natural Sciences
Seoul National University
Seoul 08826, Republic of Korea
[c] J. Won, S. Choi, Prof. M.-H. Baik
Center for Catalytic Hydrocarbon Functionalizations
Institute for Basic Science (IBS)
Daejeon 34141, Republic of Korea

Supporting information for this article is given via a link at the end of the document.

groups is achieved under exceptionally mild conditions furnishing valuable ketones as products[18] without using any external oxidant.[19] Notably, a novel substrate-assisted reaction mechanism, which commences with the aliphatic C–H activation prior to the commonly expected Ni(0/II) oxidative addition, derived from the synergistic effect of the reactivity difference between amides and aliphatic C–H bonds, is disclosed leading to a highly productive reaction pathway for the less reactive N-acylsuccinimides compared to other more activated, conventional acyl sources such as acyl chlorides or anhydrides.

Results and Discussion

Table 1. Survey of different acyl surrogates.[a]

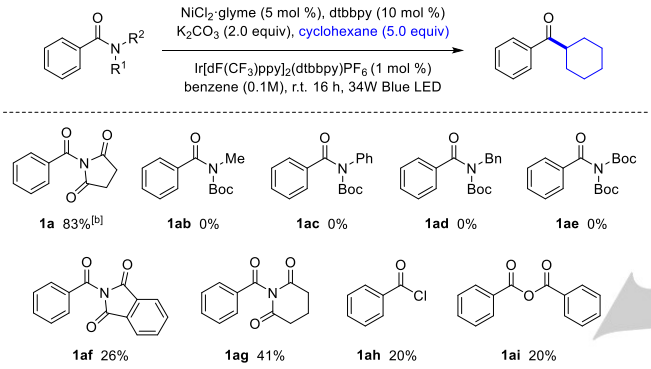

[a] Acyl surrogate (0.40 mmol), $NiCl_2$·glyme (5 mol %), dtbbpy (10 mol %), K_2CO_3 (2.0 equiv), cyclohexane (5.0 equiv), $Ir[dF(CF_3)ppy]_2(dtbbpy)PF_6$ (1 mol %), and benzene (4.0 mL) irradiated with a 34 W blue LED. Yields are determined by gas chromatography using dodecane as the internal standard. [b] Isolated yield.

Reaction Development. To design a viable catalytic system, Ni/Ir based metallaphotoredox catalytic system was deemed particularly attractive. The high proficiency of Ni(0) species to undergo oxidative addition[7b,7c,10,14b,16a,16b] and the recent advances in C–H activation mediated by the catalytic generation of a chlorine atom[18c,18e,20] under photocatalytic conditions were both considered suitable due to the high bond dissociation free energy of H–Cl (97 kcal/mol) exceeding those of simple alkanes (91 kcal/mol for cyclohexane).[18e] After assessing a variety of organic and transition-metal photosensitizers, ubiquitous iridium phenylpyridine based photocatalyst $Ir[dF(CF_3)ppy]_2(dtbbpy)PF_6$ was found to be solely effective (Table S1).[21] All reaction parameters were carefully tested, as detailed in the Supporting Information (Table S1), and the obtained results with a survey of different acyl surrogates are summarized in Table 1. N-acylsuccinimide, **1a**, was found to be an ideal coupling partner affording benzoylated cyclohexane in 83%. Interestingly, the reaction proceeded smoothly although only 5 equiv of cyclohexane was employed. Typically, significantly higher substrate concentrations were required in similar reactions that allow for directly functionalizing C(sp^3)–H bonds.[18c,19,22] Reasonable yields of 48% and 60% could be obtained even with 2 or 3 equiv of the C–H coupling partner, respectively (Table S2). Other activated amides showed diminished or no reactivity (**1ab**−**1ag**). Radical trapping experiments unambiguously demonstrated the involvement of chlorine radical and cyclohexyl radical intermediates (see the Supporting Information, Figures S1–S6).

Curiously, more activated acyl donors such as acyl chloride (**1ah**) or acyl anhydride (**1ai**), which are expected to be more susceptible to oxidative addition to the Ni center, exhibited significantly lowered reactivity compared to the less active N-acylsuccinimides. One possible explanation is that free succinimide may play a role in the catalytic cycle. Hence, control experiments were performed with **1ah** and **1ai** in the presence of 1 equiv of external succinimide, but no improvement in yield was observed (Scheme S1), implying that the enhancement of the reactivity with N-acylsuccinimides is not due to succinimide.

Mechanistic Studies. To account for the extraordinary reactivity with N-acylsuccinimides, the propensity of the acyl substrates to undergo the oxidative addition was considered first. In the case of highly reactive acyl donors such as **1ah** or **1ai**, the oxidative addition could be more facile compared to the activation of a normal C(sp^3)–H bond, i.e., the activation of **1ah** or **1ai** likely occurs prior to the C–H bond cleavage. In contrast, the significantly increased oxidative addition barrier of the C–N bond in **1a** may drive the C–H activation prior to the oxidative addition, reversing the typical sequence of the two bond breaking events. We speculated that the superior reactivity with **1a** could be ascribed to avoiding the formation of an unstable acylnickel(II) species under the "C–H activation first" pathway, enhancing the robustness of the overall catalytic cycle.

In order to check the viability of the mechanistic hypothesis, the oxidative addition complex **I** was independently prepared following the literature procedure (Scheme 2a).[18c] The acyl nickel(II) complex **I** was cautiously handled as it is easily decomposed to unidentifiable paramagnetic species even at room temperature. Previously, Shibasaki reported that an energy transfer mechanism is operative in the benzoylation of the more activated α-C–H bond in THF by irradiating complex **I** with UV light.[18c] However, in our case, the stoichiometric reaction of **I** under comparable conditions generated only a small amount (4%) of the desired acylation product with cyclohexane, demonstrating that simple energy transfer to complex **I** fails to furnish **2a** (Scheme 2a, entry 1).

As an alternative to energy transfer, a mechanism involving a single electron transfer from the oxidative addition complex **I** to engender a Ni(III) species which can produce a chlorine atom through photolysis could be possible. In order to test the capability of **I** to generate cyclohexyl bound Ni(III) species under oxidative conditions, single electron oxidants were introduced in addition to the UV irradiation (Scheme 2a, entries 2−4). Interestingly, even with the optimized Ir catalyst, **2a** was not generated efficiently, indicating that a mechanism involving the Ni(III) species is unproductive. The addition of LiCl, which may facilitate the oxidation of Ni(II) to Ni(III) by the ligation of Cl^-, still failed to deliver meaningful yields of **2a**. Overall, these experiments support that a mechanism involving **I** is not capable of producing high product yields and is not a major pathway when **1a** is used as the acyl substrate.

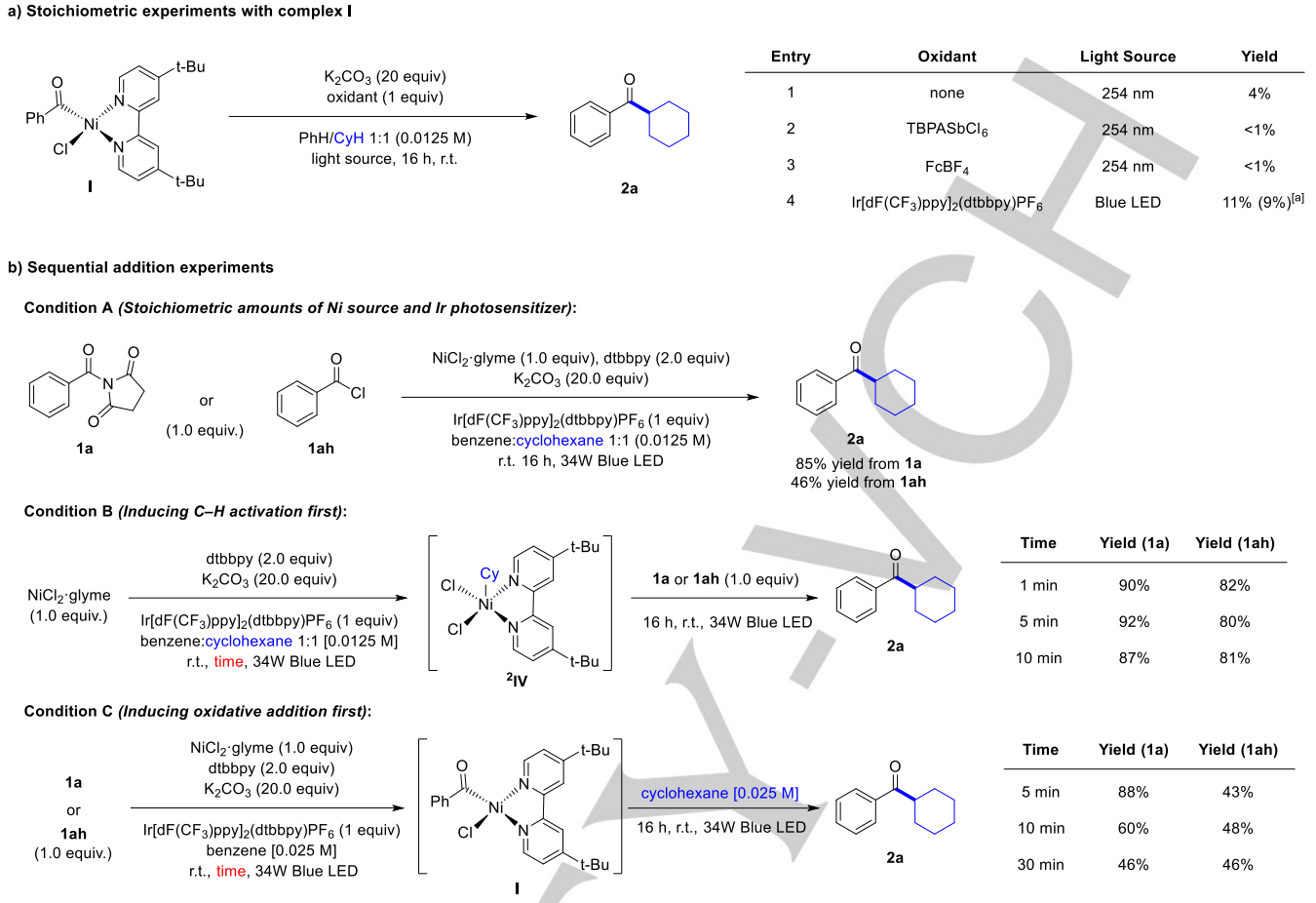

Scheme 2. Mechanistic studies. NSuc = succinimidyl, TBPA = tris(4-bromophenyl)ammoniumyl, Fc = ferrocenium. [a] With 20 equiv LiCl.

After ruling out the involvement of the oxidative addition complex **I** in the major product forming pathway, we wished to experimentally control the sequence of the two processes, oxidative addition and C−H activation. This may be achieved by varying the order of how the reaction components are added, as all redox processes should be reversible. By delayed addition of the acyl source after pre-stirring of the reaction mixture, the cyclohexyl-bound Ni species **IV** could be pre-generated, driving the reaction to the C−H activation first pathway (Scheme 2b, condition B), whereas addition of the acyl source first (condition C) will enforce the mechanism where the oxidative addition occurs first. It is therefore anticipated that **1ah** could exhibit higher performance to match that of **1a** under condition B. In contrast, the proficiency of **1a** would decrease to that of **1ah** under the condition C as the reaction is forced to undergo the oxidative addition first. Before conducting these reactions, we first verified the effects of increasing the catalyst loading on the reaction yields with stoichiometric amounts of the Ni and Ir catalysts (condition A). It was confirmed that even under such conditions, **1a** showed superior reactivity (85%) to **1ah** (46%), clearly indicating the limitations of **1ah** in the acylation reaction. Interestingly, the yield of the reaction using **1ah** was increased up to 82, 80, and 81% (cf. 90, 92, and 87% with **1a**) with 1, 5, and 10 min pre-stirring, respectively, when condition B was applied, consistently supporting the proposal of that C–H activation should be performed first to ensure high product yields. In contrast, by applying condition C, the yields from **1ah** remained constant in a range of 43–48%, while those from **1a** slowly decreased from initial 88% to 46% as the pre-stirring time increased. Although the photocatalytic reduction of Ni(II) to Ni(0) would be a slower and more endergonic process than the oxidation of Ni(II), it was clearly observed that the yield from **1a** decreased to match that from **1ah**, supporting our hypothesis that undesirable side reactions and decompositions cannot be avoided when the oxidative addition is performed first.

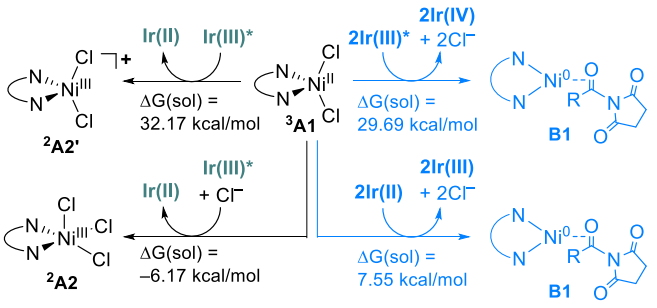

Figure 1. Possible redox pathways of the Ni(II) precatalyst.

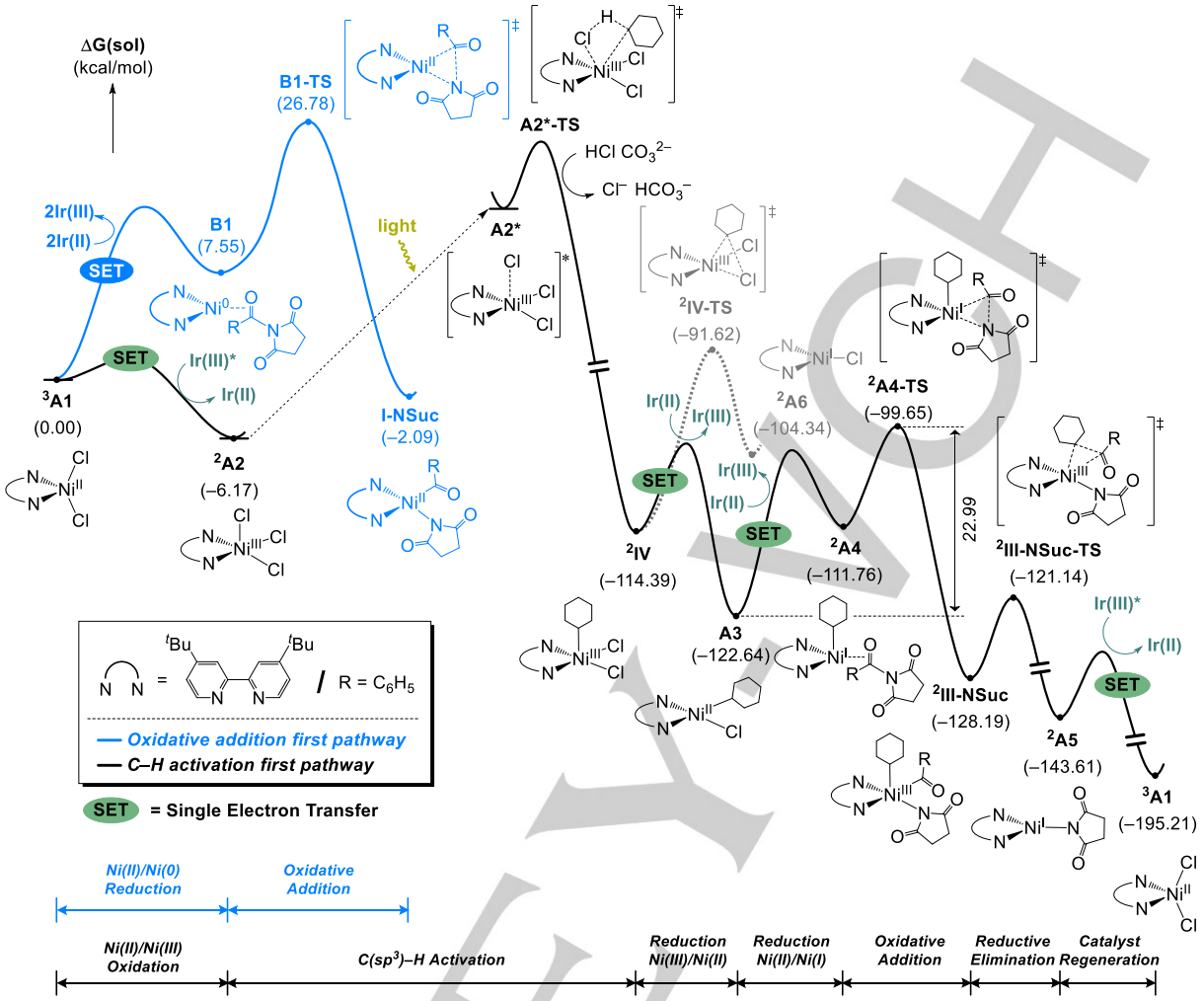

Figure 2. Free energy profile for C(sp^3)–H acylation with N-acylsuccinimide. Black trace represents C(sp^3)–H first pathway through a Ni(III) intermediate, blue trace represents oxidative addition of N-acylsuccinimide after affording Ni(0) intermediate via reduction of Ni(II).

With the strong experimental evidences of that our proposed substrate-assisted C–H first mechanism is indeed operative, we further explored various mechanistic possibilities using quantum chemical methods using density functional theory (DFT) at B3LYP-D3/cc-pVTZ(-f)[23] level of theory. Details of these calculations are given in the Supporting Information. As a starting point, to better understand which oxidation states of the Ni-complex are energetically accessible at the given reaction conditions, various possible redox processes of the Ni(II) precatalyst were calculated considering the Ir photocatalyst as a reaction partner, as summarized in Figure 1. Whereas the Ir(III)*/Ir(IV) assisted reduction to give the Ni(0) complex **B1** is 29.7 kcal/mol uphill and can therefore be safely excluded from further consideration, the oxidation of two Ir(II) species to afford the Ni(0) intermediate **B1** is viable being only 7.6 kcal/mol uphill, in good agreement with mechanisms which involves Ni(0) formation with a Ni(II) precatalyst under photocatalytic conditions.[24] Ni(III) species may be accessed directly by oxidation of the Ni(II) intermediate ^{3}**A1** mediated by Ir(III)* to form the four-coordinate tetrahedral intermediate ^{2}**A2'**, which was found to be 32.2 kcal/mol uphill in our calculations. This unrealistic energy is of course a reflection of the Ni(III) center being in a wrong coordination geometry. By adding a chloride anion a much more favorable five-coordinate, square-pyramidal Ni(III)-intermediate ^{2}**A2** can be accessed at an energy of –6.2 kcal/mol. These results indicate that both reduction and oxidation initiated pathways are feasible and must be considered. These results are in good agreement with previously reported redox potentials of Ni complex ^{3}**A1** (E^o [Ni(II)/Ni(III)] = 0.72 V, E^o [Ni(II)/Ni(0)] = –1.27 V),[20e] being well matched with the redox potentials of the Ir photocatalyst (E^o [Ir(III)*/Ir(II)] = 1.21 V, E^o [Ir(II)/Ir(III)] = –1.37 V).[25]

With the accessible Ni species identified, more detailed mechanistic calculations were performed and the key results for the reaction of N-acylsuccinimide is summarized in Figure 2. Following the conventional pathway, after formation of the Ni(0) intermediate **B1**, our calculations show that the oxidative addition step is associated with a significant barrier of 26.8 kcal/mol to give the C–N bond activation product **I-NSuc**, as illustrated in blue. Thus, under the given mild reaction conditions,

oxidative addition is found to be not competitive. On the other hand, the oxidation of **^{3}A1** to the square-pyramidal Ni(III) complex **^{2}A2** shown in black was feasible with a thermodynamic driving force of –6.2 kcal/mol. The Ni(III)-bipyridyl scaffold is photochemically competent and can absorb light in the UV-vis region to afford an Ni(III)-alkyl species **^{2}IV** traversing an excited state transition state **A2*-TS**. Unfortunately, the excited state **A2*** and the transition state **A2*-TS** cannot be located in standard DFT calculations, but these reactions are well-documented. Earlier reports by Nocera demonstrated that a LLNi(III)Cl_3 (LL = bidentate phosphine ligand) complex, which was prepared by the chemical oxidation of LLNi(II)Cl_2, extruded the molecular chorine by photon absorption.[26] The reactivity was further elaborated for C–H functionalizations through Ni/photoredox catalysis by Doyle,[18e,20b,20d] Molander,[20c] Shibasaki,[18c] Wu,[20e,20g] and Hong.[20h] Detailed electronic structure analysis of **^{2}A2** revealed significant Mulliken spin density residing on the axial chloride ligand, demonstrating the propensity of such complex to undergo the expected C–H activation process. Furthermore, time-dependent density functional theory (TD-DFT) computations regarding the Ni(III)–Cl_3 species **^{2}A2** also exhibited major relevant excitations in the blue light energy region which led to the population of apical Ni–Cl antibonding orbital (see the Supporting Information, chapter 23). As the apical chlorine takes on a radical character, the cyclohexane substrate can be engaged and a hydrogen atom extracted. Because the selectivities of C–H activation observed in this reaction are very different from what is typically observed in electrophilic radical generation methods, we propose an inner sphere σ-bond metathesis pathway for this step, as discussed below in detail.

As illustrated in Figure 2, the quenching of the newly produced excited state intermediate **A2*** accompanied by capturing the HCl with the carbonate base is highly exergonic and affords **^{2}IV**. To push the catalytic reaction forward, the Ni(III) center must be successively reduced to a Ni(I) species. First, it was reduced to a four-coordinate square-planar Ni(II) complex (**A3**) with the assistance of the Ir(II)-photosensitizer, which was shown to be energetically favorable. Interestingly, the alternative reductive elimination to form chlorocyclohexane via transition state **^{2}IV-TS** is not likely and is associated with a relatively high barrier of 22.8 kcal/mol. The productive reaction pathway continues with the consumption of reducing equivalent of Ir(II) to give the Ni(I)-alkyl complex **^{2}A4**, in which the N-acylsuccinimide coupling partner is directly bound to the nickel center. Oxidative addition via **^{2}A4-TS** with a barrier of 23.0 kcal/mol gives **^{2}III-NSuc** that can immediately undergo reductive elimination to form the desired product and **^{2}A5**. The catalytic cycle is closed by oxidizing the final Ni(I)-complex to regenerate **^{3}A1** using an equivalent of Ir(III)*. We propose that this mechanism is the major reaction pathway that consumes N-acylsuccinimides to afford over 80% product yield.

Our DFT calculations show an entirely different mechanistic possibility for the acyl chloride substrate, which is shown in Figure 3. Unlike N-acylsuccinimide, the oxidative addition of acyl chloride via the Ni(0) complex **C1** located at 13.8 kcal/mol is rapid and is predicted to occur in a nearly barrierless fashion traversing the transition state **C1-TS** found at 14.5 kcal/mol. This finding is easy to understand given the intrinsically high reactivity of acyl chloride. To push the catalysis forward, the intermediate **I** must be oxidized and a chloride ligand is recruited to give the square-pyramidal Ni(III) complex **^{2}C2** consuming an equivalent of Ir(III)*. As proposed above, this Ni(III)-bipyridyl is also photocatalytically competent and absorb light to formally produce a reactive chlorine atom that can carry out the C–H activation of the cyclohexane substrate, resulting in the Ni(II)-alkyl intermediate **^{2}C3**. Similar TD-DFT computations of **^{2}C2** also demonstrated Ni–Cl bond cleaving transitions in the blue light energy region (see the Supporting Information, chapter 23). Our calculations indicate that the reductive elimination to afford the final product and the Ni(I) intermediate **^{2}C4** is unproblematic and has a barrier of only 5.8 kcal/mol. Finally, reduction of **^{2}C4** under the consumption of an equivalent of Ir(II) additive recovers the catalytically competent Ni(0) complex **C1** to close the catalytic cycle.

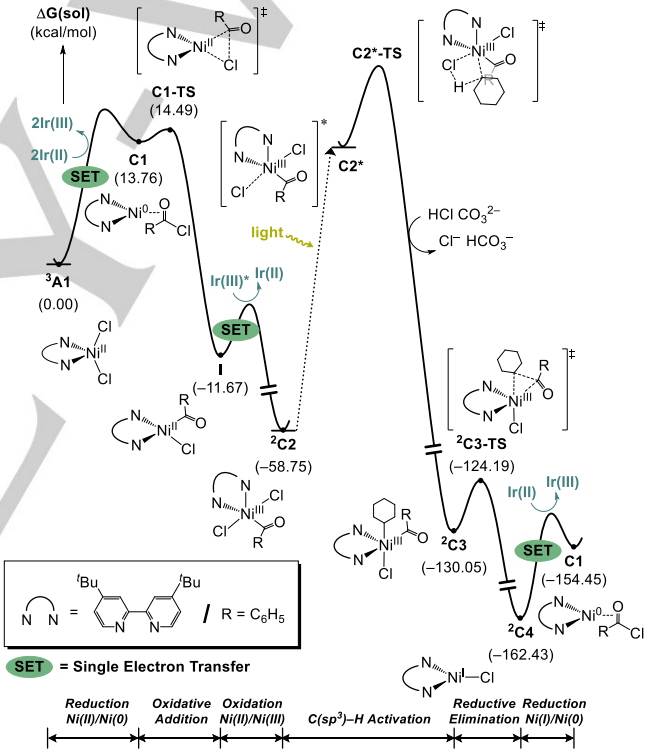

Figure 3. Reaction energy profile with acyl chloride.

In summary, our computational exploration of the various possible reaction scenarios is in full agreement with our initial mechanistic proposals and experimental studies. The non-intuitive reactivity difference of the acyl chloride and N-acylsuccinimide coupling partners originates from fundamentally different reaction pathways that these two substrates take. Whereas acyl chloride rapidly undergoes oxidative addition first due to its intrinsically high reactivity, the high barrier of oxidative addition forces N-acylsuccinimide to enter the catalytic cycle at a much later stage after the completion of the C–H activation.

Inspired by the computational investigations, we designed further control experiments from the insights obtained from the theoretically modelled mechanisms. The calculated mechanism shown in Figure 2 indicates that the reduction of the Ni(II) precursor to generate the catalytically active Ni(0) species **B1**, requires 7.6 kcal/mol. Hence, it should be possible to eliminate this step and reduce the oxidative addition barrier by this amount to 19.2 kcal/mol if a Ni(0) precursor is provided. And although such a barrier is still formidable, it is low enough, compared to 23 kcal/mol as in black traces, to bias the reaction towards initial oxidative addition even with N-acylsuccinimide substrates. Thus, we employed a Ni(0) source, $Ni(COD)_2$, in combination with substrate **1a**, as summarized in Scheme 3. Interestingly, we observed a much lower yield of 26% (entry 3), which is similar to what is seen with **1ah** and the Ni(II) precatalyst (entry 4, 20%). The addition of LiCl was essential (entry 2) as a free chloride plays a critical role in forming the photocatalytically competent species **^{2}C2** by axially coordinating to the Ni-center. The photocatalytic formal in situ oxidation of a chloride to a chlorine atom could then occur to induce hydrogen atom transfer from the cyclohexane substrate. The convergence in the reaction yields supports the hypothesis on the two underlying reactions would adapt the same mechanism. Moreover, notably, this result indicates that a Ni(0) species is not an essential component of the major catalytic cycle and can be excluded from the dominant mechanism, consistently suggesting that carrying out the oxidative addition first may not be the dominant product forming pathway to afford high yield of the acylated product.

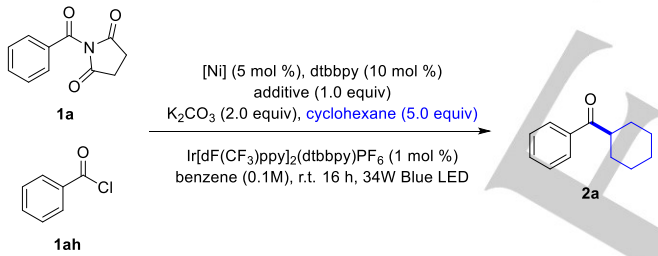

Entry	Substrate	[Ni]	Additive	Yield 2a
1	**1a**	$NiCl_2$·glyme	-	83%
2	**1a**	$Ni(COD)_2$	-	0%
3	**1a**	$Ni(COD)_2$	LiCl	26%
4	**1ah**	$NiCl_2$·glyme	-	20%

Scheme 3. Nickel precatalyst control experiments.

To gain an overall picture of the reaction profile, kinetic experiments were conducted to obtain the kinetic isotope effects (KIEs) with two different methods. Only small kinetic isotope effects were observed for both **1a** (KIE = 1.02) and **1ah** (KIE = 1.06) by standard KIE experiments of comparing the initial reaction rates of two parallel reactions with cyclohexane and cyclohexane-d_{12} (Scheme 4, method A). While the results differ from previous studies reporting primary KIEs in halogen atom mediated C–H activation reactions,[18c,18e,20c,20e] it should be noted that the reported experiments were conducted by comparing the ratios of protiated and deuterated products from an intermolecular competition reaction between protiated and deuterated C–H substrates (as in Scheme 4, method B). Although this method is a convenient way to investigate the KIEs, the experimental results should be interpreted with caution as it could provide erroneous depiction of the rate determining step; even in the cases where the rate-determining step does not involve the substrate that ultimately undergoes C–H cleavage, potential KIE could be observed in the product ratio ($[P_H]/[P_D]$) if the C–H cleavage occurs in an irreversible product-determining step.[27] Indeed, when the competition experiments between cyclohexane and cyclohexane-d_{12} were conducted, primary KIE values (**[2a]**/**[2a-*d*$_{11}$]**) of 2.13 and 2.24 were obtained with **1a** and **1ah**, respectively (Scheme 4, method B).

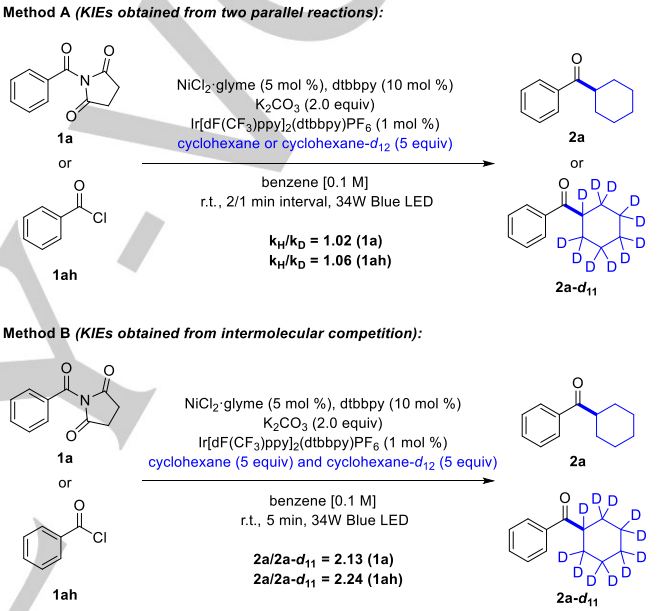

Scheme 4. Kinetic isotope effect measurements.

The observed KIEs are in good agreement with the proposed mechanisms. In the computational studies, the oxidative addition process (**A3-A4-III-NSuc**) is suggested to be the rate-limiting step for **1a**, while the initial photoreduction of **^{3}A1** to **C1** is for **1ah**, which are consistent with no primary KIEs observed with standard KIE experiments. Because the irreversible HAT-mediated C–H cleavage step could be the product-determining step under the conditions of excess cyclohexane and cyclohexane-d_{11}, pseudo-primary KIEs (**[2a]**/**[2a-*d*$_{11}$]**) were observed with method B even if a C–H cleavage is not involved in the rate-determining oxidative addition or the photoreduction process, for **1a** and **1ah**, respectively.

By combining the insights from the computational and experimental mechanistic studies, the most plausible reaction mechanism for the major pathway is proposed in Scheme 5. The initial Ni(II) precatalyst **A1** is oxidized to a Ni(III) species first, which undergoes a concerted HAT by the chlorine atom generated *in situ* under photocatalytic conditions, giving rise to

the cyclohexyl-bound Ni(III) complex **IV**. After photocatalytic reduction to Ni(I) (**A3**), oxidative addition furnishes the Ni(III) complex **III** which is subject to reductive elimination. After the reductive elimination produced the ketone product, the Ni(I) catalyst **A5** is re-oxidized to Ni(II), completing the catalytic cycle.

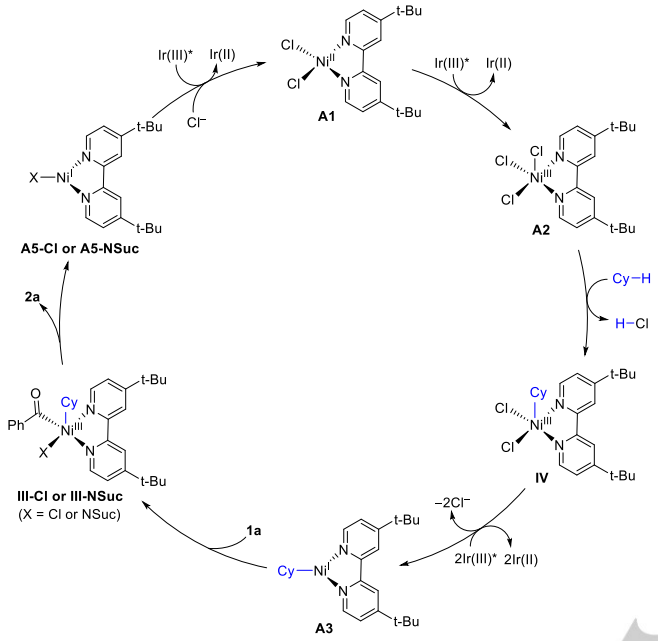

Scheme 5. Plausible reaction mechanism.

Substrate Scope Evaluation. With this clear and concrete understanding of the reaction mechanism, we moved on to investigate the substrate scope of this reaction (Table 2). Various N-benzoylsuccinimides were examined to assess the generality and functional group tolerance. While *o*-toluoylsuccinimide resulted in a modest yield (**2b**), *m*-, *p*-tolyl, and *p*-*tert*-butylphenyl groups were all tolerated (**2c**−**2e**). Reaction with acyl substrates bearing a *p*-methoxyphenyl group proceeded smoothly with no side-reaction on the hydridic α-oxy C−H bonds (**2f**). Fluorine and chlorine substituents were compatible (**2g**−**2i**). An ester-substituted aromatic group could also be employed with slightly lowered efficiency (**2j**). A sulfide group was also well-tolerated delivering the desired product in a good yield (**2k**), overcoming the issues associated with oxidation and undesired HAT. Other biologically and pharmaceutically relevant functional groups such as trifluoromethylthio (**2l**) or trifluoromethoxy (**2m**) group substituted N-succinimides also reacted smoothly. To our delight, access to dialkylketones was also possible with alkylimide substrates under the presence of various functional groups with both primary (**2o**−**2u**) and secondary (**2n**) alkyl groups. While simple primary hydrocarbon chains were successfully incorporated into the product structures (**2o**, **2p**), the functional group tolerance was evaluated with various hydrocinnamoyl moieties, proving that a wide range of functionalities including fluoro (**2q**), methoxy (**2r**), trifluoromethyl (**2s**), and cyano (**2t**) groups were adaptable. Apart from the hydrocinnamoyl moieties, functionality such as an alkoxy group directly attached to the alkyl chain was also compatible (**2u**).

In terms of the C−H coupling partner, various cyclic hydrocarbons were successfully functionalized in moderate to good yields (**2a**−**5a**). Adamantane was functionalized exclusively at the secondary position, leaving the tertiary C−H bond intact (**6a**). This is a notable feature as most previously reported HAT mediated reactions exhibited preponderance to tertiary functionalization.[28] To the best of our knowledge, the selective functionalization exclusively at the secondary position of adamantane is unprecedented for radical mediated reactions.[18e,29] This strong response to steric hindrance is likely indicative of a concerted HAT process involving the bulky Ni species[20c] in lieu of the generation of a free chlorine atom.[20b] A linear hydrocarbon, pentane, also reacted smoothly, providing a mixture of regioisomers (**7a**, α:β:γ = 1:2.25:1.25, 12% terminal after statistical correction), where a substantial amount of terminal functionalization occurred, displaying a clear contrast to the tertiary selective system reported by Nicewicz and Alexanian using the phosphatidyl radical[29] or to a similar chlorine atom mediated system reported by Doyle (1:8:4.6 ratio for pentane, 4% terminal after statistical correction).[18e] C(sp^3)−H bonds found in a norbornane type bicyclic motif were smoothly functionalized with exclusive regio- and diastereoselectivities (**8a**, **9a**) as reported in other radical involved functionalizations of norbornane type compounds due to the significantly higher bond-dissociation enthalpies of the C7–H bonds (6 kcal/mol higher than C2–H).[30] In addition to simple hydrocarbons, various ethereal C−H bonds were compatible with the developed reaction conditions (**10a**−**15a**). α-Boc-amino C(sp^3)−H bonds, which are generally inert to oxidation compared to anilines, also showed good reactivity (**16a**), proving complementary to the Doyle's previous report on α-arylamino C(sp^3)−H acylation.[18d] This finding also exemplifies that non-volatile C−H substrates could freely be incorporated without any complication in isolation processes as the required equivalences were significantly lowered compared to the previous reports and high mass-recovery of the unreacted C−H substrates could be achieved. Benzylic C−H bonds could also be acylated, albeit in moderate yields (**17a**, **18a**). Other functionalized hydrocarbons involving carbonyl groups and nitriles were also acylated on the most hydridic C−H bond with exclusive regioselectivities (**19a**−**21a**).

Table 2. Substrate scope.

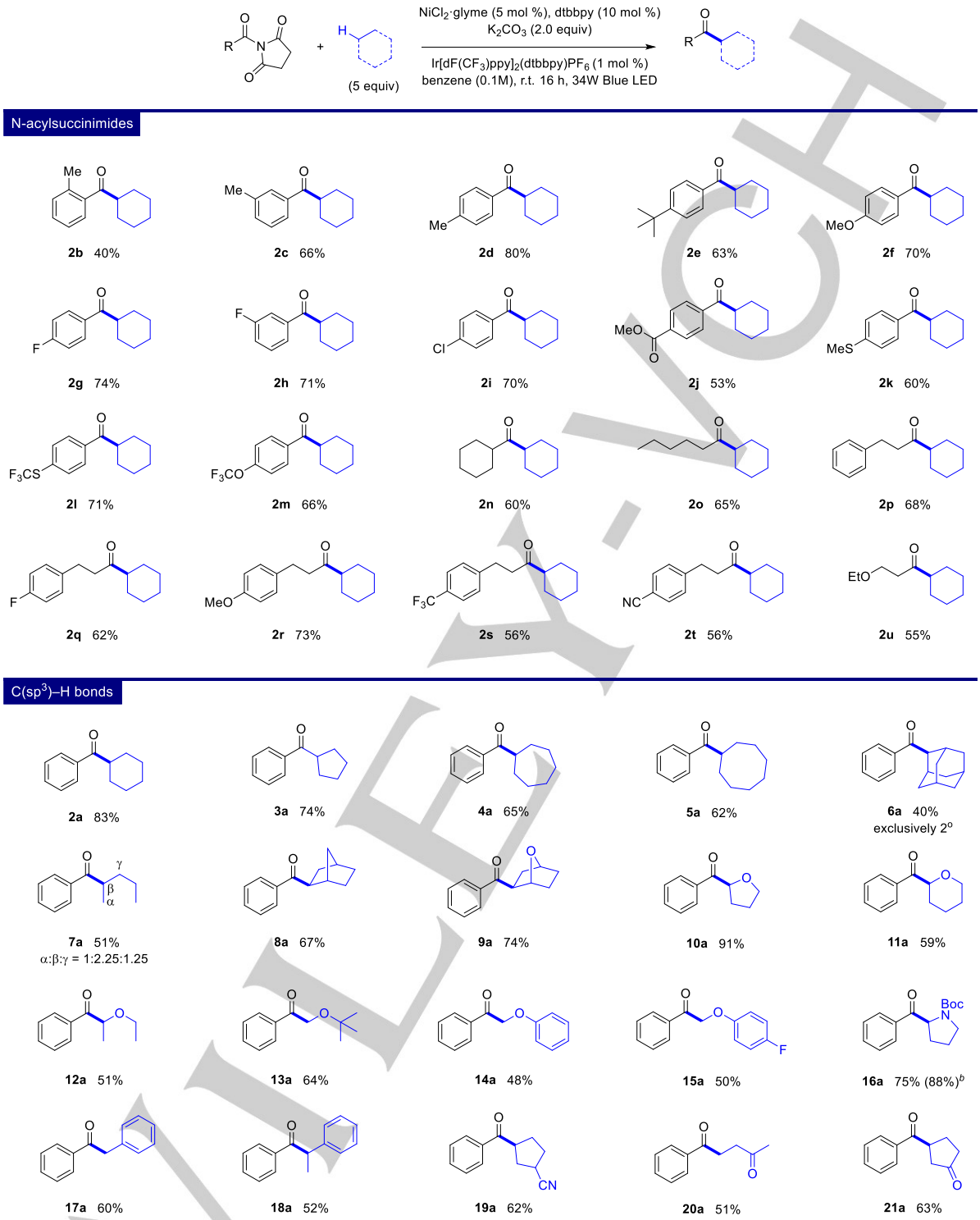

[a] Acyl surrogate (0.40 mmol), $NiCl_2$·glyme (5 mol %), dtbbpy (10 mol %), K_2CO_3 (2.0 equiv), C−H substrate (5.0 equiv), $Ir[dF(CF_3)ppy]_2(dtbbpy)PF_6$ (1 mol %), and benzene (4.0 mL) irradiated with 34 W blue LED. All yields are isolated yields. [a]Yield of recovered *N*-Boc-pyrrolidine considering 4 equiv as 100%. [b] d.r. = 2:1.

Taking advantage of high selectivity and practicality of the transformation, new efficient methods that enable direct access to a variety of biologically and chemically significant molecular structures were demonstrated (Scheme 6). As the C–H acylation reaction occurs selectively on the most hydridic position, propiophenone could be selectively acylated on the terminal primary position to directly produce a 1,4-diketone (**22a**), an extremely versatile organic building block (Scheme 6a). By

employing the classical Parr-Knorr procedures,[31] **22a** could be transformed into a series of 2,5-diaryl 5-membered heteroaromatics in good yields (**24–26**), of which the utilities span over various fields of chemistry.[32] Furthermore, double aldol condensation with phthalaldehyde furnished the naphthyl-*o*-diketone product **27**, which is a basic building block in naphtho[*c*]thiophene synthesis used for photochemical and electronic materials.[33] To our delight, the direct, selective syntheses of valuable α-amino ketone derivatives (**23a**, **16a**) were also enabled in high yields (Scheme 6b) by applying the reaction to readily available *N,N*-dimethylacetamide (DMA) and *tert*-butoxycarbonyl (Boc) protected pyrrolidine. The developed method, compared to the classical methods such as employing the organometallic addition to the Weinreb amide generated from the α-amino acid after protection,[34] could serve as an economical and convenient alternative to synthesize biologically relevant α-amino ketone products.

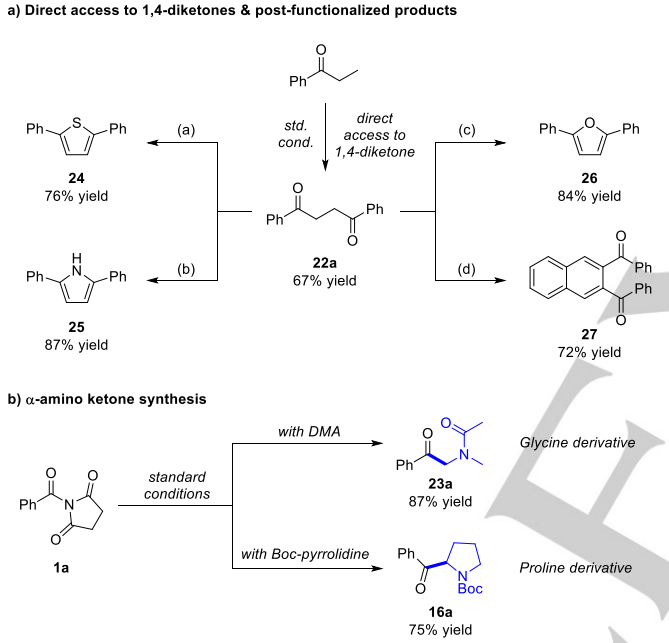

Scheme 6. Synthetic applications. (a) Lawesson's reagent (1.0 equiv), THF, 60 °C, 16 h. (b) NH_4OAc (6.0 equiv), AcOH, reflux, 16 h. (c) Ac_2O, HCl, 60 °C, 16 h. (d) phthalaldehyde (1.0 equiv), KO^{t}Bu (2.5 equiv), EtOH, r.t., 3 h. All yields are isolated yields.

Conclusion

In conclusion, an acyl transfer reaction from amides to unactivated C(sp^3)–H bonds was developed for the first time. Significant thermodynamic challenges to activate both inert bonds were overcome by careful orchestration of photoredox and Ni catalysis strategies, leading to the first merger of C(sp^3)–H functionalization and amide C–N bond cleavage. As a result, the developed condition has opened a streamlined synthetic pathway to various dialkyl and alkyl aryl ketones by coupling user-friendly amides and simple C–H substrates. Comprehensive mechanistic studies revealed that the proficiency of the N-acylsuccinimide substrate is rooted in the distinctive reaction mechanism, which involves a C–H activation event prior to the oxidative addition step, in clear contrast to the previously reported mechanisms that usually commence with the generation of an acyl nickel species by oxidative addition. This work will serve as a key starting point to further investigate the cross-sections of amide catalysis and C(sp^3)–H bond activation, enabling novel functionalization reactions which are inaccessible by traditional approaches.

Acknowledgements

This work was gratefully supported by the Samsung Science and Technology Foundation (SSTF-BA1601-12) and the Institute for Basic Science in Korea (IBS-R10-A1). We thank Prof. Sukbok Chang for insightful comments and discussions.

Keywords: C–H activation • acylation • amides • nickel • photocatalysis

[1] J. Buchspies, M. Szostak, *Catalysts* **2019**, *9*, 53-75.
[2] C. R. Kemnitz, M. J. Loewen, *J. Am. Chem. Soc.* **2007**, *129*, 2521-2528.
[3] a) C. Liu, M. Szostak, *Chem. Eur. J.* **2017**, *23*, 7157-7173; b) C. Liu, M. Szostak, *Org. Biomol. Chem.* **2018**, *16*, 7998-8010.
[4] L. Hie, N. F. Fine Nathel, T. K. Shah, E. L. Baker, X. Hong, Y.-F. Yang, P. Liu, K. N. Houk, N. K. Garg, *Nature* **2015**, *524*, 79-83.
[5] R. Takise, K. Muto, J. Yamaguchi, *Chem. Soc. Rev.* **2017**, *46*, 5864-5888.
[6] a) Y. Kajita, S. Matsubara, T. Kurahashi, *J. Am. Chem. Soc.* **2008**, *130*, 6058-6059; b) C. Liu, G. Meng, Y. Liu, R. Liu, R. Lalancette, R. Szostak, M. Szostak, *Org. Lett.* **2016**, *18*, 4194-4197; c) Y. Osumi, C. Liu, M. Szostak, *Org. Biomol. Chem.* **2017**, *15*, 8867-8871; d) G. Meng, M. Szostak, *Eur. J. Org. Chem.* **2018**, 2352-2365; e) K. S. DeGlopper, S. K. Fodor, T. B. D. Endean, J. B. Johnson, *Polyhedron* **2016**, *114*, 393-398; f) M. Rahman, J. Buchspies, M. Szostak, *Catalysts* **2019**, *9*, 129-139.
[7] a) S. Shi, R. Lalancette, R. Szostak, M. Szostak, *Org. Lett.* **2019**, *21*, 1253-1257; b) S. Shi, M. Szostak, *Org. Lett.* **2016**, *18*, 5872-5875; c) N. A. Weires, E. L. Baker, N. K. Garg, *Nat. Chem.* **2016**, *8*, 75-79; d) C. Liu, Y. Liu, R. Liu, R. Lalancette, R. Szostak, M. Szostak, *Org. Lett.* **2017**, *19*, 1434-1437; e) M. Lim, H. Kim, J. Ban, J. Son, J. K. Lee, S.-J. Min, S. U. Lee, H. Rhee, *Eur. J. Org. Chem.* **2018**, *2018*, 5717-5724.
[8] G. Meng, R. Szostak, M. Szostak, *Org. Lett.* **2017**, *19*, 3596-3599.
[9] G. Meng, R. Lalancette, R. Szostak, M. Szostak, *Org. Lett.* **2017**, *19*, 4656-4659.
[10] B. J. Simmons, N. A. Weires, J. E. Dander, N. K. Garg, *ACS Catal.* **2016**, *6*, 3176-3179.
[11] T. Zhou, C.-L. Ji, X. Hong, M. Szostak, *Chem. Sci.* **2019**, *10*, 9865-9871.
[12] S. Shi, M. Szostak, *Org. Lett.* **2017**, *19*, 3095-3098.
[13] a) Y. Liu, M. Achtenhagen, R. Liu, M. Szostak, *Org. Biomol. Chem.* **2018**, *16*, 1322-1329; b) G. Li, T. Zhou, A. Poater, L. Cavallo, S. P. Nolan, M. Szostak, *Catal. Sci. Technol.* **2020**, *10*, 710-716; c) S. Yu, T. Shin, M. Zhang, Y. Xia, H. Kim, S. Lee, *Org. Lett.* **2018**, *20*, 7563-7566.
[14] a) S. Shi, M. Szostak, *ACS Omega* **2019**, *4*, 4901-4907; b) J. Hu, Y. Zhao, J. Liu, Y. Zhang, Z. Shi, *Angew. Chem. Int. Ed.* **2016**, *55*, 8718-8722.
[15] a) A. Dey, S. Sasmal, K. Seth, G. K. Lahiri, D. Maiti, *ACS Catal.* **2016**, *7*, 433-437; b) H. Yue, L. Guo, S. C. Lee, X. Liu, M. Rueping, *Angew. Chem. Int. Ed.* **2017**, *56*, 3972-3976.
[16] a) C. Liu, M. Szostak, *Chem. Commun.* **2018**, *54*, 2130-2133; b) C. Liu, M. Szostak, *Angew. Chem. Int. Ed.* **2017**, *56*, 12718-12722; c) C. Li, P. Li, J. Yang, L. Wang, *Chem. Commun.* **2012**, *48*, 4214-4216; d) H. Yue, L. Guo, H. H. Liao, Y. Cai, C. Zhu, M. Rueping, *Angew. Chem. Int. Ed.*

2017, *56*, 4282-4285. e) J. Chen, M. Xu, S. Yu, Y. Xia, S. Lee, *Org. Lett.* **2020**, *22*, 2287-2292.

[17] J. Amani, R. Alam, S. Badir, G. A. Molander, *Org. Lett.* **2017**, *19*, 2426-2429.

[18] a) J. Amani, E. Sodagar, G. A. Molander, *Org. Lett.* **2016**, *18*, 732-735; b) J. Amani, G. A. Molander, *J. Org. Chem.* **2017**, *82*, 1856-1863; c) Z. Sun, N. Kumagai, M. Shibasaki, *Org. Lett.* **2017**, *19*, 3727-3730; d) C. L. Joe, A. G. Doyle, *Angew. Chem. Int. Ed.* **2016**, *55*, 4040-4043; e) L. K. G. Ackerman, J. I. Martinez Alvarado, A. G. Doyle, *J. Am. Chem. Soc.* **2018**, *140*, 14059-14063; f) T. Yano, T. Kawasaki, T. Yuhki, N. Ishida, M. Murakami, *Org. Lett.* **2018**, *20*, 1224-1227; g) Y. Masuda, N. Ishida, M. Murakami, *Chem. Asian. J.* **2019**, *14*, 403-406.

[19] X. Zhang, Z. Wang, X. Fan, J. Wang, *J. Org. Chem.* **2015**, *80*, 10660-10667.

[20] a) K. Ohkubo, A. Fujimoto, S. Fukuzumi, *Chem. Commun.* **2011**, *47*, 8515-8517; b) B. J. Shields, A. G. Doyle, *J. Am. Chem. Soc.* **2016**, *138*, 12719-12722; c) D. R. Heitz, J. C. Tellis, G. A. Molander, *J. Am. Chem. Soc.* **2016**, *138*, 12715-12718; d) M. K. Nielsen, B. J. Shields, J. Liu, M. J. Williams, M. J. Zacuto, A. G. Doyle, *Angew. Chem. Int. Ed.* **2017**, *129*, 7297-7300; e) H.-P. Deng, X.-Z. Fan, Z.-H. Chen, Q.-H. Xu, J. Wu, *J. Am. Chem. Soc.* **2017**, *139*, 13579-13584; f) P. Mondal, P. Pirovano, A. Das, E. R. Farquhar, A. R. McDonald, *J. Am. Chem. Soc.* **2018**, *140*, 1834-1841; g) H. P. Deng, Q. Zhou, J. Wu, *Angew. Chem. Int. Ed.* **2018**, *57*, 12661-12665; h) S. Y. Go, G. S. Lee, S. H. Hong, *Org. Lett.* **2018**, *20*, 4691-4694.

[21] a) L. N. Cavalcanti, G. A. Molander, *Top. Curr. Chem.* **2016**, *374*, 39; b) J. C. Tellis, C. B. Kelly, D. N. Primer, M. Jouffroy, N. R. Patel, G. A. Molander, *Acc. Chem. Res.* **2016**, *49*, 1429-1439; c) J. Twilton, C. Le, P. Zhang, M. H. Shaw, R. W. Evans, D. W. C. MacMillan, *Nat. Rev. Chem.* **2017**, *1*, 0052; d) C. K. Prier, D. A. Rankic, D. W. C. MacMillan, *Chem. Rev.* **2013**, *113*, 5322-5363; e) K. L. Skubi, T. R. Blum, T. P. Yoon, *Chem. Rev.* **2016**, *116*, 10035-10074.

[22] D. Liu, C. Liu, H. Li, A. Lei, *Angew. Chem. Int. Ed.* **2013**, *52*, 4453-4456.

[23] a) C. Lee, W. Yang, R. G. Parr, *Phys. Rev. B Condens. Matter* **1988**, *37*, 785-789; b) S. Grimme, J. Antony, S. Ehrlich, H. Krieg, *J. Chem. Phys.* **2010**, *132*, 154104; c) T. H. Dunning, *J. Chem. Phys.* **1989**, *90*, 1007-1023.

[24] Z.-H. Qi, J. Ma, *ACS Catal.* **2018**, *8*, 1456-1463.

[25] M. S. Lowry, J. I. Goldsmith, J. D. Slinker, R. Rohl, R. A. Pascal, G. G. Malliaras, S. Bernhard, *Chem. Mater.* **2005**, *17*, 5712-5719.

[26] a) S. J. Hwang, B. L. Anderson, D. C. Powers, A. G. Maher, R. G. Hadt, D. G. Nocera, *Organometallics* **2015**, *34*, 4766-4774; b) S. J. Hwang, D. C. Powers, A. G. Maher, B. L. Anderson, R. G. Hadt, S.-L. Zheng, Y.-S. Chen, D. G. Nocera, *J. Am. Chem. Soc.* **2015**, *137*, 6472-6475.

[27] E. M. Simmons, J. F. Hartwig, *Angew. Chem. Int. Ed.* **2012**, *51*, 3066-3072.

[28] L. P. Ermolenko, C. Giannotti, *J. Chem. Soc. Perkin Trans. 2* **1996**, 1205-1210.

[29] K. A. Margrey, W. L. Czaplyski, D. A. Nicewicz, E. J. Alexanian, *J. Am. Chem. Soc.* **2018**, *140*, 4213-4217.

[30] a) P. M. Nunes, S. G. Estacio, G. T. Lopes, B. J. Costa Cabral, R. M. Borges dos Santos, J. A. Martinho Simões, *Org. Lett.* **2008**, *10*, 1613-1616; b) I. B. Perry, T. F. Brewer, P. J. Sarver, D. M. Schultz, D. A. DiRocco, D. W. C. MacMillan, *Nature* **2018**, *560*, 70-75.

[31] J. Xuan, Z.-J. Feng, J.-R. Chen, L.-Q. Lu, W.-J. Xiao, *Chem. Eur. J.* **2014**, *20*, 3045-3049.

[32] a) R. Mishra, K. K. Jha, S. Kumar, I. Tomer, *Der. Pharma. Chemica.* **2011**, *3*, 38-54; b) R. Mishra, P. K. Sharma, *Int. J. Eng. Al. Sci.* **2015**, *1*, 46-59; c) A. Al-Mulla, *Der. Pharma. Chemica.* **2019**, *9*, 141-147; d) G. Barbarella, M. Melucci, G. Sotgiu, *Adv. Mater.* **2005**, *17*, 1581-1593; e) C. Oliver Kappe, S. Shaun Murphree, A. Padwa, *Tetrahedron* **1997**, *53*, 14179-14233; f) D. J. Shrinivas, A. M. Uttam, H. K. Venkatrao, M. A. Tejraj, *Cur. Org. Chem.* **2013**, *17*, 2279-2304; g) R. Banerjee, H. K. S. Kumar, M. Banerjee, *Int. J. Rev. Life. Sci.* **2012**, *1*, 46-59.

[33] J. A. Clement, A. K. Mohanakrishnan, *Tetrahedron* **2010**, *66*, 2340-2350.

[34] a) R. K. Dieter, R. R. Sharma, H. Yu, V. K. Gore, *Tetrahedron* **2003**, *59*, 1083-1094; b) D. P. Mahajan, H. M. Godbole, G. P. Singh, G. G. Shenoy, *J. Chem. Sci.* **2019**, *131*, 22.

10.1002/anie.202004441

WILEY-VCH

RESEARCH ARTICLE

A synergistic activation of amides and hydrocarbons, both thermodynamically stable, was achieved to enable direct C(sp^3)–H acylation through nickel/photoredox catalysis. Comprehensive mechanistic studies indicate an unusual mechanism where the C–H activation occurs prior to the oxidative addition to form Ni(I)-alkyl species which is critical for reaction efficiencies.

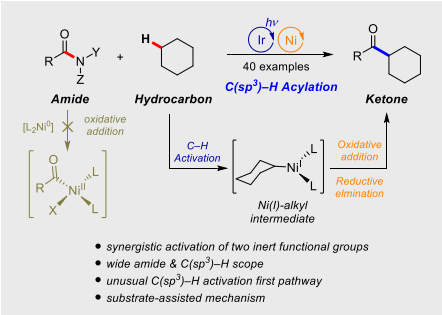

Geun Seok Lee, Joonghee Won, Seulhui Choi, Mu-Hyun Baik, and Soon Hyeok Hong**

Page No. – Page No.

Synergistic Activation of Amides and Hydrocarbons for Direct C(sp^3)–H Acylation Enabled by Metallaphotoredox Catalysis